

Aqueous Chemistry of (2,2',2''-Terpyridine)gold(III). Preparation and Structures of [Au(terpy)Cl]Cl₂·3H₂O and the Mixed-Valence Au(I)-Au(III) Salt [Au(terpy)Cl]₂[AuCl₂]₃[AuCl₄]

L. Steven Hollis and Stephen J. Lippard*

Contribution from the Department of Chemistry, Columbia University,
New York, New York 10027. Received November 15, 1982

Abstract: The reaction of tetrachloroauric acid (HAuCl₄) with 2,2',2''-terpyridine (terpy) in aqueous solution provides a good yield of the potential metallointercalator [Au(terpy)Cl]Cl₂·3H₂O. Amber crystals of this product were found by single-crystal X-ray diffraction methods to contain the planar cation [Au(terpy)Cl]²⁺, weakly associated with axial chloride (Au...Cl = 3.05 Å) and water (Au...O = 3.02 Å) ligands. These weak axial interactions are lacking in related Pt(II) and Pd(II) metallointercalation reagents, suggesting that the DNA binding properties of the new gold complex might be different. The Au-N bond lengths in [Au(terpy)Cl]²⁺ are inequivalent, with the Au-N distance trans to the chlorine atom being 0.09 Å shorter than the equivalent distance of 2.03 Å found for the two nitrogen atoms cis to chlorine. A secondary product of the reaction, which crystallizes under acidic conditions as purple-red needles, was found by X-ray diffraction to be the mixed-valence complex [Au(terpy)-Cl]₂[AuCl₂]₃[AuCl₄]. This insoluble compound contains three linear [AuCl₂]⁻ anions, arranged in a spiral (Au-Au distance = 3.09 Å), which link two [Au(terpy)Cl]²⁺ cations through axial sites [Au(III)-Au(I) distance = 3.30 Å]. The remaining axial site of each [Au(terpy)Cl]²⁺ cation is occupied by a chlorine atom from a square-planar [AuCl₄]⁻ anion at a distance of 3.40 Å. Each of the [AuCl₄]⁻ anions bridges two [Au(terpy)Cl]²⁺ cations resulting in a polymeric ...Cl-Au(III)-Cl...Au(III)...Au(I)...Au(I)...Au(I)...Au(III)...Cl-Au(III)-Cl... chain.

Metallointercalation reagents such as [Pt(terpy)X]⁺, where terpy = 2,2',2''-terpyridine and X = Cl⁻ or RS⁻, have been used extensively to investigate the binding of intercalators to DNA and as probes for studying the structure of nucleic acids.¹⁻¹⁰ Related planar, cationic platinum(II) complexes of 1,10-phenanthroline and 2,2'-bipyridine also bind to DNA by intercalation,¹¹ and recently tris(*o*-phenanthroline)zinc(II) was found to exhibit enantiomeric selectivity in its intercalative binding to DNA.¹² Apart from platinum and palladium,¹³ metallointercalation reagents based on other square-planar, d⁸ transition-metal complexes have not been investigated. In this study we have examined the reaction between tetrachloroauric acid (HAuCl₄) and terpyridine in order to prepare a potential gold metallointercalation reagent, [Au(terpy)Cl]²⁺. The chemistry of gold in aqueous solution is of current interest because of recently intensified research on gold-containing antiarthritic and antineoplastic drugs.¹⁴⁻¹⁶

The reactions of Au(III) amine complexes have been investigated in the course of important kinetic and mechanistic work that helped to elucidate ligand substitution processes in square-planar transition-metal complexes.¹⁷⁻²⁰ While the chemistry of Au(III) complexes containing tridentate amine ligands, such as diethylenetriamine (dien)^{18,19} or substituted diethylenetriamines,^{20,21} of the form [Au(triamine)X]²⁺ (where X = halide) is well established, the chemistry of the related [Au(terpy)X]²⁺ complexes has remained undeveloped. The aqueous chemistry of Au(III) complexes is typically complicated by pH-dependent hydrolysis reactions which often lead to reduction.¹⁴ Au(III) complexes that contain tridentate ligands such as dien, however, are quite stable in aqueous solutions. Since the tridentate terpyridine ligand is also likely to stabilize the Au(III) oxidation state, we chose to examine the chemistry of [Au(terpy)Cl]²⁺. Such a stable gold metallointercalation reagent would resemble [Pt(terpy)Cl]⁺ but, because of its different charge, would be expected to have different DNA binding properties.

In this report we show that [Au(terpy)Cl]Cl₂·3H₂O can be prepared in high yield from the reaction of HAuCl₄ with terpyridine in water. We also report the structures of this complex and of a mixed-valence Au(I)-Au(III) compound obtained as a byproduct of the reaction. The mixed-valence complex is a novel salt composed of a chainlike assembly of [Au(terpy)Cl]²⁺, [Au-

Cl₂]⁻, and [AuCl₄]⁻ units which crystallize out of solution in a 2:3:1 ratio. The relationship between this and other Au(I) and Au(III) compounds is also examined.

Experimental Section and Results

Preparation of Compounds. All gold complexes were prepared from HAuCl₄·3H₂O (Mallinckrodt) and 2,2',2''-terpyridine (Sigma Chemical Co.). Elemental analyses were performed by Galbraith Laboratories,

- (1) Lippard, S. J. *Acc. Chem. Res.* **1978**, *11*, 211.
- (2) Jennette, K. W.; Lippard, S. J.; Vassiliades, G. A.; Bauer, W. R. *Proc. Natl. Acad. Sci. U.S.A.* **1974**, *71*, 3839.
- (3) Jennette, K. W.; Gill, J. T.; Sadownick, J. A.; Lippard, S. J. *J. Am. Chem. Soc.* **1976**, *98*, 6159.
- (4) Barton, J. K.; Lippard, S. J. *Biochemistry* **1979**, *18*, 2661.
- (5) Howe-Grant, M.; Lippard, S. J. *Biochemistry* **1979**, *18*, 5762.
- (6) Bond, P. J.; Langridge, R.; Jennette, K. W.; Lippard, S. J. *Proc. Natl. Acad. Sci. U.S.A.* **1975**, *72*, 4825.
- (7) Strothkamp, K. G.; Lippard, S. J. *Proc. Natl. Acad. Sci. U.S.A.* **1976**, *73*, 2536.
- (8) Wong, Y. S.; Lippard, S. J. *J. Chem. Soc., Chem. Commun.* **1977**, 824.
- (9) Wang, A. H.; Nathans, J.; van der Marel, G.; van Boom J. H.; Rich, A. *Nature (London)* **1978**, *276*, 471.
- (10) Wang, A. H.; Quigley, G. J.; Kolpak, F. J.; Rich, A. *Abstr. Am. Crystallogr. Assoc.* **1979**, *6*, 50.
- (11) Lippard, S. J.; Bond, P. J.; Wu, K. C.; Bauer, W. R. *Science (Washington, D.C.)* **1976**, *194*, 726.
- (12) Barton, J. K.; Dannenberg, J. J.; Raphael, A. L. *J. Am. Chem. Soc.* **1982**, *104*, 4967.
- (13) Howe-Grant, M.; Wu, K. C.; Bauer, W. R.; Lippard, S. J. *Biochemistry* **1976**, *15*, 4339.
- (14) Shaw, C. F., III *Inorg. Persp. Biol. Med.* **1979**, *2*, 287.
- (15) Sadler, P. J. *Struct. Bonding (Berlin)* **1976**, *29*, 171.
- (16) (a) Sutton, B. M. *ACS Symp. Ser.* **1983**, *No. 209*, 355. (b) Razi, M. T.; Otiko, G.; Sadler, P. J. *Ibid.* **1983**, *No. 209*, 371. (c) Elder, R. C.; Eidsness, M. K.; Heeg, M. J.; Tepperman, K. G.; Shaw, C. F., III; Schaeffer, N. *Ibid.* **1983**, *No. 209*, 385. (d) Brown, D. H.; Smith, W. E. *Ibid.* **1983**, *No. 209*, 401.
- (17) Basolo, F.; Pearson, R. G. "Mechanisms of Inorganic Reactions", 2nd ed.; Wiley: New York, **1967**; pp 382-416.
- (18) (a) Baddley, W. H.; Basolo, F. *Inorg. Chem.* **1964**, *3*, 1087. (b) Baddley, W. H.; Basolo, F.; Gray, H. B.; Nörling, C.; Poë A. J. *Ibid.* **1963**, *2*, 921.
- (19) Nardin, G.; Randaccio, L.; Annibale, G.; Natile, G.; Pitteri, B. *J. Chem. Soc., Dalton Trans.* **1980**, 220.
- (20) Weick, C. F.; Basolo, F. *Inorg. Chem.* **1966**, *5*, 576.
- (21) Annibale, G.; Natile, G.; Cattalini, L. *J. Chem. Soc., Dalton Trans.* **1976**, 1547.

* Address correspondence to this author at the Department of Chemistry, Massachusetts Institute of Technology, Cambridge, MA 02139.

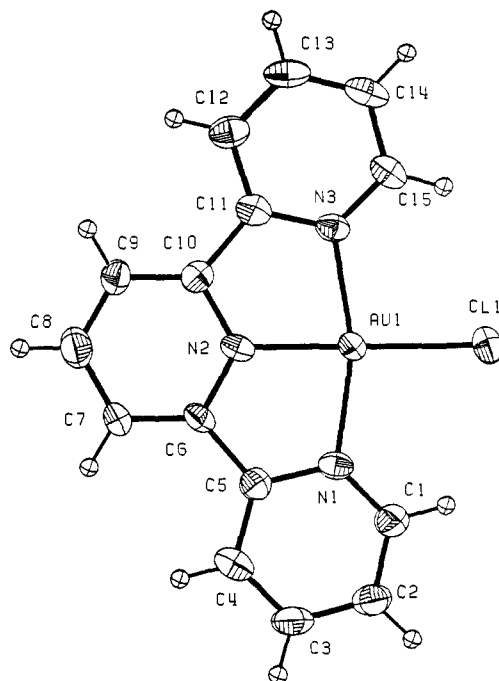


Figure 1. ORTEP illustration of the structure of the divalent cation, $[\text{Au}(\text{terpy})\text{Cl}]^{2+}$ (1), showing the 40% probability thermal ellipsoids. For clarity the hydrogen atoms are depicted as spheres with B set to 1 \AA^2 . The hydrogen atom labels (not shown) are assigned according to the atom to which they are attached.

Knoxville, TN, and Schwarzkopf Microanalytical Laboratory, Woodside, NY. Proton NMR spectra were obtained at 90 MHz by using a Bruker R-32 continuous-wave spectrometer.

$[\text{Au}(\text{terpy})\text{Cl}]_2\text{Cl}_2 \cdot 3\text{H}_2\text{O}$ (1). Several products were obtained from the reaction of HAuCl_4 with terpyridine, depending upon the initial pH of the solution. The best yields of compound 1 were obtained in the pH range $3 \leq \text{pH} \leq 5$, using the following method. A mixture of 0.97 g (2.5 mmol) of $\text{HAuCl}_4 \cdot 3\text{H}_2\text{O}$ and 0.633 g (2.7 mmol) of terpyridine was placed in 75 mL of water, and the pH of the solution was adjusted to 3.0 with 1 N NaOH. The resulting mixture, a yellow-orange solution and a purple solid, was brought to reflux temperature and within 1.5 h the solid dissolved, producing a dark red solution. After being refluxed for 24 h, the solution was filtered to remove small amounts of a purple solid and the filtrate was evaporated to dryness under reduced pressure. Recrystallization from water provided 1.16 g (2 mmol) of compound 1 (80% yield). The amber crystals of $[\text{Au}(\text{terpy})\text{Cl}]_2\text{Cl}_2 \cdot 3\text{H}_2\text{O}$ lose water upon standing in air. After the crystals were air-dried, the chemical analysis data best fit the formula $[\text{Au}(\text{terpy})\text{Cl}]_2\text{Cl}_2 \cdot 2.5\text{H}_2\text{O}$. Anal. Calcd for $\text{Au}_2\text{C}_{15}\text{H}_{16}\text{N}_3\text{Cl}_3\text{O}_{2.5}$: Au, 33.86; C, 30.97; H, 2.77; N, 7.22; Cl, 18.29. Found: Au, 33.9; C, 30.76; H, 2.78; N, 7.18; Cl, 18.63. ^1H NMR (in D_2O , shifts measured relative to HOD at δ 4.75 vs. Me_4Si and reported vs. Me_4Si) δ 9.27 (d, $\text{H}_1, \text{H}_{15}$), 8.67 (m, H_3-H_{13}), 8.14 (m, $\text{H}_2, \text{H}_{14}$). The numbering scheme is given in Figure 1.

The yield of compound 1 decreased when the initial pH of the reaction was adjusted outside of the range 3–5. With pH greater than 6, the product of the reaction was gold metal. When the pH of the solution was unadjusted (pH 1.9) or raised slightly (to pH 2.5), a number of insoluble tetrachloroaurate salts were obtained. Two of these products have been identified, $[\text{Au}(\text{terpy})\text{Cl}]_2[\text{AuCl}_2]_3[\text{AuCl}_4]$ and $[\text{Hterpy}][\text{H}_2\text{terpy}][\text{AuCl}_4]_3$, and their preparation is discussed below.

$[\text{Au}(\text{terpy})\text{Cl}]_2[\text{AuCl}_2]_3[\text{AuCl}_4]$ (2). Dark purple needles of compound 2 were obtained in small yields (15–20 mg) from the reaction used to prepare compound 1, as described above. This insoluble complex crystallized during the reflux step and was separated from the solution by filtration. Its composition was determined crystallographically (vide infra). Small amounts of this complex were also found to be intermixed with the $[\text{AuCl}_4]^-$ salt of terpyridine when the initial pH of the solution was kept low ($1.9 < \text{pH} < 3$).

$[\text{Hterpy}][\text{H}_2\text{terpy}][\text{AuCl}_4]_3$ (3). The tetrachloroaurate salt of protonated terpyridine, 3, was obtained as the primary product from the reaction of HAuCl_4 and terpyridine when the initial pH was adjusted between 2 and 3. The detailed procedure is as follows. A mixture of 0.97 g (2.5 mmol) of $\text{HAuCl}_4 \cdot 3\text{H}_2\text{O}$ and 0.58 g (2.5 mmol) of terpyridine was suspended in 60 mL of water and heated to reflux for 24 h. The resulting red-amber solution was separated from a yellow insoluble precipitate by

Table I. Experimental Details of the X-ray Diffraction Studies of $[\text{Au}(\text{terpy})\text{Cl}]_2\text{Cl}_2 \cdot 3\text{H}_2\text{O}$ (1) and $[\text{Au}(\text{terpy})\text{Cl}]_2[\text{AuCl}_2]_3[\text{AuCl}_4]$ (2)

	1	2
(A) Crystal Parameters ^a at 23 °C		
a , Å	8.4576 (7)	9.703 (1)
b , Å	7.084 (2)	15.351 (1)
c , Å	31.246 (3)	7.813 (1)
α , deg	90	92.05 (1)
β , deg	94.748 (7)	106.58 (1)
γ , deg	90	107.102 (9)
space group	$P2_1/c$	$P\bar{1}$
Z	4	1
ρ (calcd), g cm^{-3}	2.102	3.258
ρ (obsd), g cm^{-3}	2.10 (2) ^b	3.24 (2) ^c
mol wt	590.6	2073.8
vol, Å ³	1865.6	1056.8
(B) Measurement of Intensity Data ^d		
radiation	Mo $K\alpha$	graphite monochromatized
(λ , Å)	0.710 73 Å	
standards, ^e measured	($\bar{3}, \bar{2}, 7$), ($\bar{4}, 1, 8$), ($\bar{4}, 6, 0$), ($1, \bar{7}, 3$),	
every 1 h of X-ray	($3, 4, 10$)	($4, 4, 1$)
exposure time		
no. of reflections	4995 [$3 < 2\theta$	5521 [$3 < 2\theta < 55^\circ$
collected (non	$< 55^\circ$ ($\pm h$,	($\pm h, \pm k, +l$), [$3 <$
space group	$+k, +l$]	$2\theta < 20^\circ$ ($\pm h, \pm k, -l$)]
extinguished)		
(C) Treatment of Intensity Data ^f		
μ , cm^{-1}	77.12	199.28
transmission	0.21–0.38	0.21–0.51
factor range		
average, R_{av} ^d	0.032	0.021
no. of reflections	4291	4806
after averaging		
obsd unique data	3362	3274
$[F_o > 4\sigma(F_o)]$		

^a From a least-squares fit of the setting angles of 25 reflections with $2\theta > 30^\circ$. ^b By suspension in a mixture of CHBr_3 and CHCl_3 . ^c By suspension in an aqueous solution of thallose formate. ^d See ref 23 for further details. ^e Showed no decay. ^f F_o and $\sigma(F_o)$ were corrected for background, attenuator, and Lorentz-polarization of X-radiation as described previously (see ref 23).

filtration. The filtrate was rotoevaporated to dryness and washed with water, 2-propanol, and ether. The combined yield of the yellow insoluble salt was 0.69 g (52%). Anal. Calcd for $\text{Au}_3\text{C}_{30}\text{H}_{25}\text{N}_6\text{Cl}_{12}$: C, 24.25; H, 1.70; N, 5.66; Cl, 28.63. Found: C, 24.11; H, 1.67; N, 5.60; Cl, 28.63.

Reaction of compound 3 with aqueous base produced $[\text{Au}(\text{terpy})\text{Cl}]_2\text{Cl}_2 \cdot 3\text{H}_2\text{O}$ (1) in good yield. A 110-mg sample of compound 3 was suspended in 10 mL of water and heated to 60°C , after the pH was adjusted to 6.0 with 1 N NaOH. The yellow solid dissolved after 1 h, producing an orange-rose solution. The solution was cooled and filtered, and the filtrate was rotoevaporated to dryness. Recrystallization of this sample provided 70 mg of 1 (62%).

Collection and Reduction of X-ray Data. **$[\text{Au}(\text{terpy})\text{Cl}]_2\text{Cl}_2 \cdot 3\text{H}_2\text{O}$ (1).** An amber crystal of compound 1 was sealed in a capillary tube to avoid dehydration. The crystal was tabular in shape with dimensions of 0.23 mm \times 0.25 mm \times 0.17 mm and was bounded by the following faces: (100), ($\bar{1}00$), (001), ($00\bar{1}$), (011), ($\bar{1}\bar{1}\bar{2}$). The quality of the crystal was examined by taking open counter ω scans of several strong low-angle reflections and was found to be acceptable ($\Delta\omega_{1/2} \approx 0.1^\circ$). The unit-cell parameters and intensity data were measured with a single-crystal diffractometer as described in Table I. The space group was determined to be $P2_1/c$ (C_{2h}^5 , No. 14)²² from the systematic absences. Further details of the data collection and reduction are given in Table I and ref 23.

$[\text{Au}(\text{terpy})\text{Cl}]_2[\text{AuCl}_2]_3[\text{AuCl}_4]$ (2). The purple crystal used in the diffraction study was a needle with dimensions of 0.32 mm \times 0.08 mm \times 0.03 mm and was bounded by the faces (100), ($\bar{1}00$), (010), ($0\bar{1}0$), (001), ($30\bar{1}$). Several low-angle ω scans indicated the crystal to be acceptable for data collection ($\Delta\omega_{1/2} = 0.1^\circ$). The space group was determined to be either $P\bar{1}$ (C_1^1 , No. 2) or $P1$ (C_1^1 , No. 1).²⁴ The former

(22) "International Tables for X-ray Crystallography", 3rd ed., Kynoch Press: Birmingham, England, 1973; Vol. I, p 99.

(23) Silverman, L. D.; Dewan, J. C.; Giandomenico, C. M.; Lippard, S. J. *Inorg. Chem.* 1980, 19, 3379.

Table II. Final Positional Parameters for [Au(terpy)Cl]Cl₂·3H₂O (1)^a

ATOM	X	Y	Z
Au1	0.28766(3)	0.36284(4)	0.423500(10)
Cl1	0.2113(3)	0.3704(4)	0.49138(8)
Cl2	0.4321(3)	0.7549(3)	0.41660(7)
Cl3	-0.0591(3)	1.0733(4)	0.30298(8)
N1	0.5052(7)	0.2450(9)	0.4361(2)
N2	0.3474(7)	0.3434(8)	0.3653(2)
N3	0.0898(7)	0.4734(9)	0.3927(2)
C1	0.5752(10)	0.2037(13)	0.4746(3)
H1	0.5219(10)	0.2291(13)	0.4996(3)
C2	0.7235(11)	0.1250(13)	0.4786(3)
H2	0.7731(11)	0.0964(13)	0.5063(3)
C3	0.8009(11)	0.0871(14)	0.4423(4)
H3	0.9038(11)	0.0325(14)	0.4448(4)
C4	0.7288(10)	0.1285(11)	0.4028(3)
H4	0.7813(10)	0.1031(11)	0.3777(3)
C5	0.5772(9)	0.2085(12)	0.3994(3)
C6	0.4886(8)	0.2640(11)	0.3588(3)
C7	0.5306(10)	0.2425(13)	0.3174(3)
H7	0.6299(10)	0.1891(13)	0.3119(3)
C8	0.4248(11)	0.3005(16)	0.2842(3)
H8	0.4511(11)	0.2847(16)	0.2555(3)
C9	0.2820(11)	0.3809(12)	0.2918(3)
H9	0.2102(11)	0.4201(12)	0.2684(3)
C10	0.2439(9)	0.4040(10)	0.3333(3)
C11	0.0991(9)	0.4815(11)	0.3494(3)
C12	-0.0237(10)	0.5628(13)	0.3239(4)
H12	-0.0168(10)	0.5743(13)	0.2938(4)
C13	-0.1564(11)	0.6270(12)	0.3424(4)
H13	-0.2430(11)	0.6781(12)	0.3248(4)
C14	-0.1636(10)	0.6175(12)	0.3853(4)
H14	-0.2538(10)	0.6641(12)	0.3981(4)
C15	-0.0374(9)	0.5387(11)	0.4106(3)
H15	-0.0417(9)	0.5313(11)	0.4409(3)
O1	0.1227(8)	-0.0025(12)	0.3972(3)
O2	0.4911(8)	0.7846(14)	0.3196(3)
O3	0.2231(9)	0.8655(12)	0.2845(3)

^a Atoms are labeled as shown in Figure 1. The hydrogen atoms of the terpyridine ring are labeled according to carbon atoms to which they are attached.

choice, suggested on the basis of statistical tests,²⁵ was confirmed by the successful solution and refinement of the structure. Further details of the data collection and reduction are presented in Table I.

Structure Solution and Refinement

[Au(terpy)Cl]Cl₂·3H₂O (1). The structure solved by standard Patterson and Fourier methods and refined²⁶ by using anisotropic thermal parameters for all non-hydrogen atoms and a set of common isotropic thermal parameters for all hydrogen atoms. Neutral atom scattering factors and anomalous dispersion corrections for non-hydrogen atoms were obtained from ref 27, and hydrogen atom scattering factors were taken from ref 28. The positions of all terpyridine ring hydrogen atoms were placed at calculated positions, $d(\text{C-H}) = 0.95 \text{ \AA}$, and constrained to "ride" on the carbon atoms to which they are attached.²⁴ The hydrogen atoms attached to the water molecules of hydration were not located.

Full-matrix least-squares refinement of the structure using 227 parameters converged at $R_1 = 0.044$ and $R_2 = 0.058$.²⁹ The function minimized during the refinement was $\sum w(|F_o| - |F_c|)^2$, where $w = 1.4465/[\sigma^2(F_o) + 0.000625(F_o)^2]$. The maximum parameter shift per sd in the final cycle of refinement was 0.1, and the largest peaks in the final difference Fourier map were less than $1.0 \text{ e } \text{\AA}^{-3}$, and these peaks were in the vicinity ($\leq 1.1 \text{ \AA}$) of the Au atom. The average $w\Delta^2$ values for groups of data sectioned according to parity group, $(\sin \theta)/\lambda$, $|F_o|$, $|h|$, $|k|$, or $|l|$, showed good consistency, and the weighting scheme was considered to be acceptable.

The final atomic positional parameters, together with their estimated standard deviations, are reported in Table II. The interatomic distances and angles with estimated standard deviations are presented in Table IV. A complete listing of atomic positional and thermal parameters for compound 1 (Table S1) and a complete listing of observed and calculated

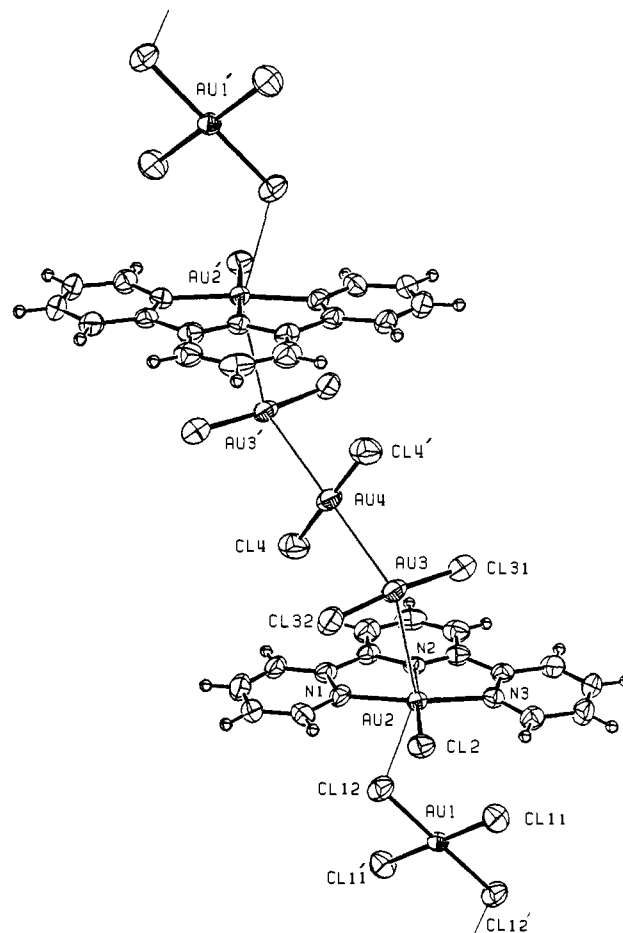


Figure 2. ORTEP illustration of the structure of the mixed-valent complex [Au(terpy)Cl]₂[AuCl₂]₃[AuCl₄] (2), showing the extended chainlike relationship between the AuCl₄⁻, AuCl₂⁻, and [Au(terpy)Cl]²⁺ units. The long contacts (>3.0 Å) between the Au(I) and Au(III) units are indicated with light lines. The crystallographically unique portion of the structure is comprised by the unprimed atoms shown in the figure. The gold atoms Au1 and Au4 lie on crystallographic inversion centers, and all primed atoms are related to the unprimed atoms through inversion symmetry. The labels of the carbon and hydrogen atoms of the [Au(terpy)Cl]²⁺ cation (not shown) are assigned as described in compound 1 (see Figure 1). All non-hydrogen atoms are shown with 40% probability thermal ellipsoids, and hydrogen atoms are depicted as spheres with B set to 1 \AA^2 .

structure factors (Table S3) are available as supplementary material. Figure 1 shows the structure and atom labeling scheme of the [Au(terpy)Cl]²⁺ cation.

[Au(terpy)Cl]₂[AuCl₂]₃[AuCl₄] (2). The positions of the four independent Au atoms in the unit cell were located using MULTAN.²⁵ Two of the Au atoms (Au1 and Au4) lie on crystallographic inversion centers. As a consequence, the unique portion of the structure is half of that given above, [Au(terpy)Cl][AuCl₂]_{1.5}[AuCl₄]_{0.5}. A difference Fourier map, phased on the Au atoms, provided the positions of all non-hydrogen atoms. The structure was refined as described above with anisotropic thermal parameters for all non-hydrogen atoms and the hydrogen atoms were refined with constraints using a set of common isotropic thermal parameters for all hydrogen atoms of the terpyridine ring.

Full-matrix least-squares refinement of the structure using 248 parameters converged at $R_1 = 0.032$ and $R_2 = 0.039$.²⁹ The weighting function used in the refinement was $w = 1.0119/[\sigma^2(F_o) + 0.000625(F_o)^2]$, and the maximum parameter shift in the final cycle of refinement was 0.001σ . The only residual peaks of significant height ($\leq 1.7 \text{ e } \text{\AA}^{-3}$) that were observed in the final difference Fourier map were near the Au atoms ($\leq 1.1 \text{ \AA}$). The $w\Delta^2$ values for groups of data, sectioned as above, showed good consistency, and the weighting scheme was found to be acceptable.

The final atomic positional parameters with their estimated standard deviations are reported in Table III. The interatomic distances with estimated standard deviations are presented in Table V. A complete listing of atomic positional and thermal parameters for compound 2

(24) Reference 22, pp 74, 75.

(25) Germain, G.; Main, P.; Woolfson, M. M. *Acta Crystallogr., Sect. A* **1971**, *A27*, 368.

(26) All calculations were performed on a DEC VAX-11/780 computer using SHELX-76: Sheldrick, G. M. In "Computing in Crystallography"; Schenk, H., Olthof-Hazekamp, R., van Koningsveld, H., Bassi, G. C., Eds; Delft University Press: Delft, The Netherlands 1978; pp 34-42.

(27) "International Tables for X-ray Crystallography"; Kynoch Press: Birmingham, England, 1974; Vol. IV, pp 99, 149.

(28) Stewart, R. F.; Davidson, E. R.; Simpson, W. T. *J. Chem. Phys.* **1965**, *42*, 3175.

(29) $R_1 = \sum |F_o| - |F_c| / \sum |F_o|$; $R_2 = [\sum w(|F_o| - |F_c|)^2 / \sum w|F_o|^2]^{1/2}$.

Table III. Final Positional Parameters for $[\text{Au}(\text{terpy})\text{Cl}]_2[\text{AuCl}_2]_3[\text{AuCl}_4] (2)^a$

ATOM	X	Y	Z
Au1	0.0000	0.0000	0.0000
Au2	0.72154(4)	0.19420(3)	0.16537(5)
Au3	0.55436(6)	0.34582(3)	0.22856(6)
Au4	0.5000	0.5000	0.0000
Cl2	0.5716(3)	0.08652(19)	0.2807(4)
Cl4	0.4424(4)	0.5553(2)	0.2357(6)
Cl11	0.0004(4)	0.0388(3)	-0.7165(4)
Cl12	-0.1838(4)	0.0645(2)	-0.1162(5)
Cl31	0.8006(4)	0.4316(2)	0.3639(5)
Cl32	0.3119(4)	0.2495(3)	0.1140(4)
N1	0.5749(9)	0.1821(6)	-0.0851(11)
N2	0.8532(9)	0.2847(5)	0.0658(11)
N3	0.9114(9)	0.2311(6)	0.3804(12)
C1	0.4308(11)	0.1243(8)	-0.1494(16)
H1	0.3868(11)	0.0873(8)	-0.0718(16)
C2	0.3484(14)	0.1195(9)	-0.3261(16)
H2	0.2481(14)	0.0779(9)	-0.3716(16)
C3	0.4126(15)	0.1757(10)	-0.4357(17)
H3	0.3549(15)	0.1710(10)	-0.5584(17)
C4	0.5546(14)	0.2366(9)	-0.3736(15)
H4	0.5964(14)	0.2760(9)	-0.4496(15)
C5	0.6368(12)	0.2381(7)	-0.1948(14)
C6	0.7951(12)	0.2993(7)	-0.1072(14)
C7	0.8887(15)	0.3624(9)	-0.1770(18)
H7	0.8531(15)	0.3746(9)	-0.2973(18)
C8	1.0346(15)	0.4092(8)	-0.0713(20)
H8	1.0984(15)	0.4539(8)	-0.1199(20)
C9	1.0911(13)	0.3931(8)	0.1049(18)
H9	1.1921(13)	0.4251(8)	0.1773(18)
C10	0.9948(12)	0.3283(7)	0.1718(16)
C11	1.0293(11)	0.2979(7)	0.3502(14)
C12	1.1671(12)	0.3320(8)	0.4891(18)
H12	1.2482(12)	0.3797(8)	0.4715(18)
C13	1.1823(13)	0.2965(9)	0.6472(17)
H13	1.2764(13)	0.3198(9)	0.7415(17)
C14	1.0669(13)	0.2281(9)	0.6748(17)
H14	1.0800(13)	0.2024(9)	0.7848(17)
C15	0.9300(12)	0.1949(8)	0.5362(15)
H15	0.8475(12)	0.1479(8)	0.5523(15)

^a Atoms are labeled as shown in Figure 2. The atom labels of the carbon and hydrogen atoms of the terpyridine ligand are numbered as shown in compound 1.

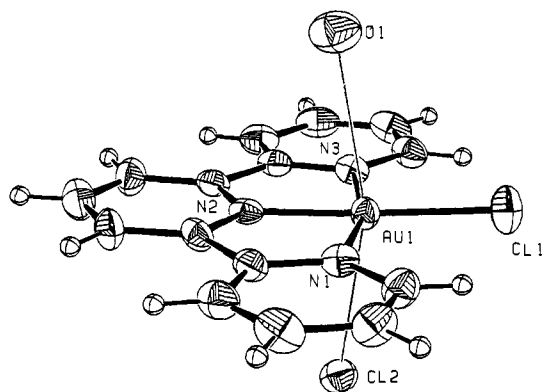


Figure 3. ORTEP illustration of the $[\text{Au}(\text{terpy})\text{Cl}]^{2+}$ cation in **1** showing the axial ligand contacts to Cl2 and water molecule O1. The carbon and hydrogen atom labels are omitted for clarity (see Figure 1 caption).

(Table S2) and a listing of final observed and calculated structure factors (Table S4) are available as supplementary material. Figure 2 shows the coordination geometry and atom labeling scheme for compound **2**.

Discussion

Description of the Structures. $[\text{Au}(\text{terpy})\text{Cl}]\text{Cl}_2 \cdot 3\text{H}_2\text{O}$ (**1**). ORTEP illustrations of the $[\text{Au}(\text{terpy})\text{Cl}]^{2+}$ cation are shown in Figures 1 and 3. The coordination geometry of the gold atom is distorted slightly from that found in normal square-planar Au(III) complexes. While the $[\text{Au}(\text{terpy})\text{Cl}]^{2+}$ cation is planar (the root-mean-square deviation of the 17 non-hydrogen atoms from the plane is 0.033 Å), the bond angles between the adjacent donor atoms in the plane deviate significantly from 90° (Table IV). The Au–N bond lengths within the cation are also inequivalent, with the Au–N distance trans to Cl1 being 0.09 Å (9σ)³⁰ shorter than the Au–N distances found for the two nitrogen atoms cis to Cl1. A similar distorted square-planar geometry,

(30) The esd is calculated using $\sigma = (\sigma_1^2 + \sigma_2^2)^{1/2}$, where σ_1 and σ_2 are the errors in the bond lengths or angles being compared.

Table IV. Interatomic Distances (Å) and Angles (deg) for $[\text{Au}(\text{terpy})\text{Cl}]\text{Cl}_2 \cdot 3\text{H}_2\text{O}$ (**1**)^a

Coordination Sphere			
Au–N1	2.029(6)	Au–Cl1	2.269(2)
Au–N2	1.931(7)	Au–Cl2	3.049(2)
Au–N3	2.018(6)	Au–O1	3.022(8)
N1–Au–N2	81.4(3)	N3–Au–O1	81.8(2)
N2–Au–N3	81.4(3)	Cl1–Au–O1	96.5(2)
N1–Au–Cl1	98.7(2)	N1–Au–Cl2	91.5(2)
N2–Au–Cl1	176.9(2)	N2–Au–Cl2	82.0(2)
N3–Au–Cl1	98.5(2)	N3–Au–Cl2	86.2(2)
N1–Au–N3	162.7(3)	Cl1–Au–Cl2	101.0(1)
N1–Au–O1	95.2(2)	O1–Au–Cl2	160.0(2)
N2–Au–O1	80.4(2)		
Ligand Geometry			
N1–C1	1.329(11)	C5–C6	1.471(11)
N1–C5	1.367(10)	C6–C7	1.390(11)
N2–C6	1.351(9)	C7–C8	1.374(13)
N2–C10	1.345(10)	C8–C9	1.374(13)
N3–C11	1.362(11)	C9–C10	1.373(11)
N3–C15	1.336(9)	C10–C11	1.469(10)
C1–C2	1.369(12)	C11–C12	1.381(12)
C2–C3	1.384(15)	C12–C13	1.381(13)
C3–C4	1.361(15)	C13–C14	1.350(15)
C4–C5	1.398(11)	C14–C15	1.392(13)
Au–N1–C1	126.5(6)	N3–C11–C10	116.3(7)
Au–N1–C5	112.0(5)	N3–C11–C12	119.2(7)
C1–N1–C5	121.5(7)	N3–C15–C14	120.4(9)
N1–C1–C2	120.6(9)	C1–C2–C3	119.7(9)
N1–C5–C4	118.8(8)	C2–C3–C4	119.7(9)
N1–C5–C6	116.2(7)	C3–C4–C5	119.7(9)
Au–N2–C6	118.3(5)	C4–C5–C6	124.9(8)
Au–N2–C10	118.2(5)	C5–C6–C7	128.8(7)
C6–N2–C10	123.4(7)	C6–C7–C8	118.2(8)
N2–C6–C5	112.0(7)	C7–C8–C9	121.4(9)
N2–C6–C7	119.1(7)	C8–C9–C10	119.4(8)
N2–C10–C9	118.5(7)	C9–C10–C11	129.5(8)
N2–C10–C11	112.0(7)	C10–C11–C12	124.5(8)
Au–N3–C11	112.1(5)	C11–C12–C13	119.6(10)
Au–N3–C15	126.8(6)	C12–C13–C14	120.2(9)
C11–N3–C15	121.1(7)	C13–C14–C15	119.3(8)

Possible Hydrogen Bonds

O1–Cl2 ^a	= 3.147(8)	O2–Cl2	= 3.120(9)
O1–Cl3	= 3.251(9)	O3–Cl3	= 3.128(9)
O2–O3	= 2.79(1)	O3–Cl3	= 3.189(9)

^a See Figure 1 for atom labeling scheme. Bond distances have not been corrected for thermal motion.

which is a result of the steric requirements of the terpyridine ligand, also occurs in the related terpyridine complexes of palladium(II) and platinum(II), $[\text{Pd}(\text{terpy})\text{Cl}]\text{Cl}_2 \cdot 2\text{H}_2\text{O}$,³¹ $[\text{Pt}(\text{terpy})(\text{SC}_2\text{H}_4\text{OH})](\text{NO}_3)_2$,³ and $[\text{Pt}(\text{terpy})\text{Cl}]_2[\text{PtCl}_4]$.³² The Au–N bond lengths in compound **1** are comparable to the Au–N distances (1.97–2.14 Å) found in other four-coordinate Au(III) amine complexes, such as $[\text{Au}(\text{dien})\text{Cl}]^{2+}$ ¹⁹ and $[\text{Au}(\text{en})(\text{SO}_3)_2]^-$,³³ the Au–Cl bond distance [2.269 (2) Å] is within the 2.26–2.42 Å range normally found for Au–Cl bonds in Au(III) complexes.^{19,34} The geometry of the terpyridine ligand is also normal.³ As shown in Figure 3, space above and below the planar cation is occupied by a chloride anion (Cl2) and a water molecule of hydration (O1). Although the Au–Cl2 and Au–O1 distances of 3.049 (2) and 3.022 (8) Å, respectively, are longer than normal Au–Cl (~2.27 Å)^{19,34} and Au–O (~2.04 Å)³⁵ bond lengths, they are much shorter than the usual nonbonded contacts between these atoms (4.0 Å for Au–Cl and 3.6 Å for Au–O).¹⁹ A similar situation occurs in the structure of $[\text{Au}(\text{dien})\text{Cl}](\text{Cl})(\text{ClO}_4)$,¹⁹ in which the planar $[\text{Au}(\text{dien})\text{Cl}]^{2+}$ cation has an axial chloride anion [$d(\text{Au}–\text{Cl}) = 3.05$ Å] and an axial oxygen atom from the ClO_4^- group [$d(\text{Au}–\text{O}) = 3.10$ Å].

A stereoview of the unit-cell packing of compound **1** is shown in Figure 4. The cations in the unit cell are oriented in the lattice with their planes oriented roughly parallel ($\pm 24^\circ$) to the (010)

(31) Intille, G. M.; Pfluger, C. E.; Baker, W. A., Jr. *J. Cryst. Mol. Struct.* **1973**, *3*, 47.

(32) Intille, G. M. Ph.D. Dissertation, Syracuse University, Syracuse, NY, 1967.

(33) Dunand, A.; Gerdil, R. *Acta Crystallogr., Sect. B* **1975**, *B31*, 370.

(34) Robinson, W. T.; Sinn, E. *J. Chem. Soc., Dalton Trans.* **1975**, 726.

(35) Jones, P. G.; Rumpel, H.; Schwarzmann, E.; Sheldrick, G. M.; Paulus, H. *Acta Crystallogr., Sect. B* **1979**, *B35*, 1435.

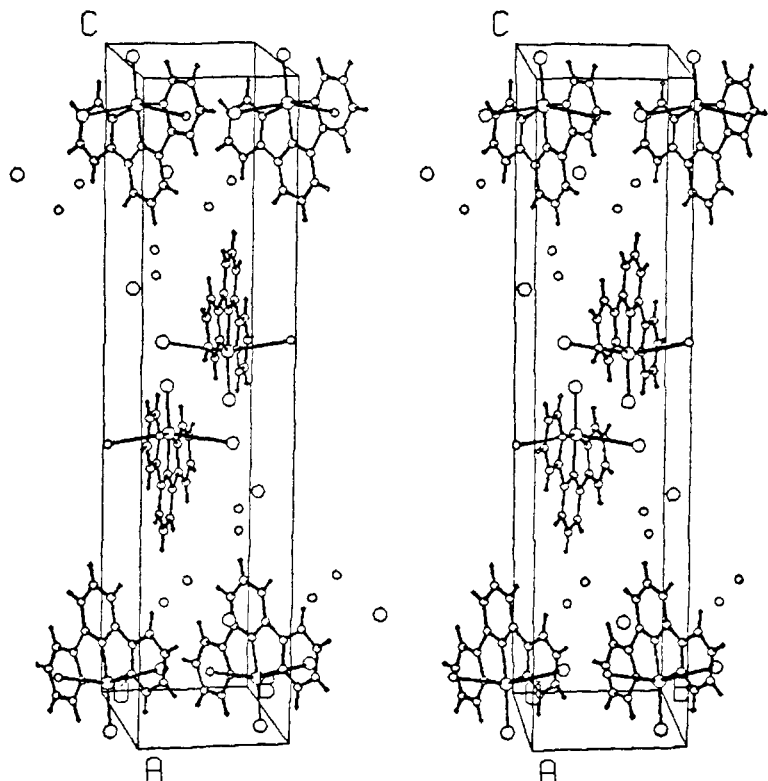


Figure 4. Stereoview of the unit-cell packing diagram for $[\text{Au}(\text{terpy})\text{Cl}]\text{Cl}_2 \cdot 3\text{H}_2\text{O}$ (1). The long axial contacts to Cl2 and O1 are shown as solid lines.

Table V. Interatomic Distances (Å) and Angles (deg) for $[\text{Au}(\text{terpy})\text{Cl}]\text{Cl}_2 \cdot 3\text{H}_2\text{O}$ (1)

Coordination Spheres			
Au1-Cl11	2.271(3)	Au2-Cl12	3.401(4)
Au1-Cl12	2.272(3)	Au2-Au3	3.2997(8)
Au2-N1	2.030(8)	Au3-Cl31	2.273(3)
Au2-N2	1.941(8)	Au3-Cl32	2.276(4)
Au2-N3	2.022(9)	Au3-Au4	3.0932(5)
Au2-Cl2	2.259(3)	Au4-Cl4	2.276(4)
Cl11-Au1-Cl12	90.5(1)	N1-Au2-Au3	79.2(3)
Cl11-Au1-Cl12'	89.5(1)	N2-Au2-Au3	89.4(3)
Au1-Cl12-Au2	119.4(1)	N3-Au2-Au3	102.7(3)
N1-Au2-N2	81.4(4)	Cl2-Au2-Au3	91.99(9)
N2-Au2-N3	81.3(4)	Cl12-Au2-Au3	150.01(6)
N1-Au2-Cl2	99.0(3)	Cl31-Au3-Cl32	174.0(1)
N2-Au2-Cl2	178.6(2)	Cl31-Au3-Au2	89.4(1)
N3-Au2-Cl2	98.3(3)	Cl32-Au3-Au2	96.6(1)
N1-Au2-N3	162.6(4)	Cl31-Au3-Au4	90.98(9)
N1-Au2-Cl12	72.7(3)	Cl32-Au3-Au4	94.9(1)
N2-Au2-Cl12	76.4(3)	Au2-Au3-Au4	128.31(2)
N3-Au2-Cl12	101.1(3)	Cl4-Au4-Au3	85.3(1)
Cl1-Au2-Cl12	102.4(1)		
Ligand Geometry			
N1-C1	1.353(13)	C5-C6	1.488(15)
N1-C5	1.370(13)	C6-C7	1.365(15)
N2-C6	1.363(12)	C7-C8	1.376(17)
N2-C10	1.398(12)	C8-C9	1.389(19)
N3-C11	1.378(13)	C9-C10	1.380(15)
N3-C15	1.343(14)	C10-C11	1.464(15)
C1-C2	1.370(15)	C11-C12	1.400(14)
C2-C3	1.381(18)	C12-C13	1.355(16)
C3-C4	1.356(17)	C13-C14	1.370(18)
C4-C5	1.392(14)	C14-C15	1.392(15)
Au2-N1-C1	126.6(8)	N3-C11-C10	115.1(9)
Au2-N1-C5	113.2(7)	N3-C11-C12	118.9(11)
C1-N1-C5	120.1(9)	N3-C15-C14	120.5(11)
N1-C1-C2	120.0(12)	C1-C2-C3	119.4(12)
N1-C5-C4	121.2(10)	C2-C3-C4	122.0(12)
N1-C5-C6	114.8(9)	C3-C4-C5	117.3(12)
Au2-N2-C6	117.7(7)	C4-C5-C6	123.9(10)
Au2-N2-C10	117.7(7)	C5-C6-C7	129.7(10)
C6-N2-C10	124.5(9)	C6-C7-C8	119.6(12)
N2-C6-C5	112.7(9)	C7-C8-C9	121.9(12)
N2-C6-C7	117.4(11)	C8-C9-C10	117.5(12)
N2-C10-C9	119.1(11)	C9-C10-C11	127.5(11)
N2-C10-C11	113.4(9)	C10-C11-C12	126.0(10)
Au2-N3-C11	112.5(7)	C11-C12-C13	119.4(11)
Au2-N3-C15	126.5(8)	C12-C13-C14	121.5(11)
C11-N3-C15	121.0(9)	C13-C14-C15	118.7(12)

^a See Figure 2 for the atom labeling scheme. Bond distances have not been corrected for thermal motion.

plane. The chlorine anion (Cl3) and the water molecules of hydration (O2 and O3) are packed in channels between the planar cations. A listing of the possible hydrogen bonds is given in Table IV. The axial water molecule O1 has short contacts to the chloride anion Cl3 and to the axial chlorine atom (Cl2) of an adjacent cation (see the bottom pair of cations in Figure 4). The two water molecules of hydration also appear to be hydrogen bonded to one another [$d(\text{O2}-\text{O3}) = 2.79$ (1) Å]. These water molecules also have additional short contacts to the axial chlorine atom (O2-Cl2) and to the lattice chloride anion (O3-Cl3).

$[\text{Au}(\text{terpy})\text{Cl}]\text{Cl}_2 \cdot 3\text{H}_2\text{O}$ (2). This mixed-valent compound crystallizes such that two of the four crystallographically independent gold atoms (Au1 and Au4) lie on inversion centers (Figure 2). Three $[\text{AuCl}_2]^-$ anions, arranged in a spiral, bridge two $[\text{Au}(\text{terpy})\text{Cl}]^{2+}$ cations through long axial contacts. The distance between the Au3 atom in the linear $[\text{AuCl}_2]^-$ anion, and the axial site of the Au2 atom in the $[\text{Au}(\text{terpy})\text{Cl}]^{2+}$ cation is 3.300 (1) Å. The other axial position of the $[\text{Au}(\text{terpy})\text{Cl}]^{2+}$ cation is occupied by chlorine atom Cl12 of the $[\text{AuCl}_4]^-$ anion at distance of 3.401 (4) Å. An infinite chain of gold containing anions and cations is thereby generated (Figure 2).

With the exception of the axial site contacts, the geometry of the $[\text{Au}(\text{terpy})\text{Cl}]^{2+}$ cation is nearly identical with that found in the structure of compound 1. The $[\text{Au}(\text{terpy})\text{Cl}]^{2+}$ cation in compound 2 is planar (the root-mean-square deviation of all non-hydrogen atoms from the plane is 0.046 Å), and the Au2 atom is displaced slightly (0.098 Å) from the plane toward Au3.

The square-planar geometry of the $[\text{AuCl}_4]^-$ anion and the linear geometry of the $[\text{AuCl}_2]^-$ anions in compound 2 are typical for complexes of Au(III) and Au(I), respectively. The Au-Cl bond lengths and the Cl-Au-Cl bond angles in the planar $[\text{AuCl}_4]^-$ anion are equivalent to those found in the structure of $\text{K}[\text{AuCl}_4] \cdot 2\text{H}_2\text{O}$.³⁶ The $[\text{AuCl}_4]^-$ anion in compound 2 is required by crystallographic symmetry to be planar since it lies on an inversion center. The linear $[\text{AuCl}_2]^-$ anions also have Au-Cl bond distances and angles comparable to those found in a number of structures of complexes containing this anion.³⁷⁻³⁹

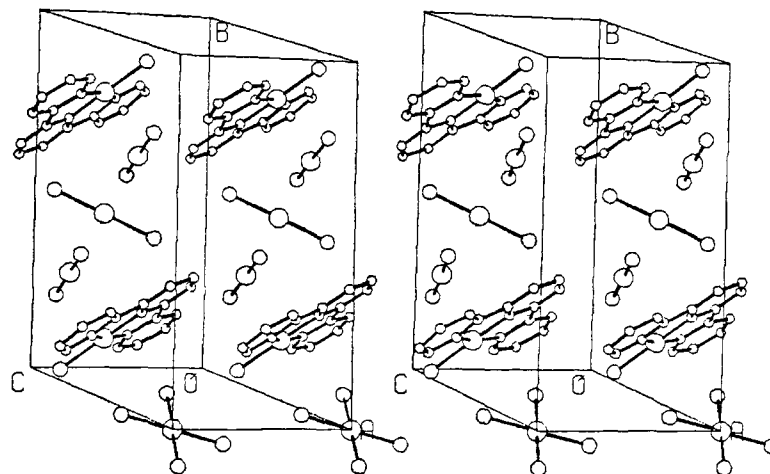


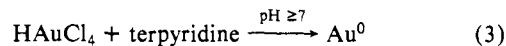
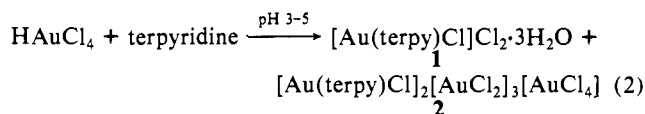
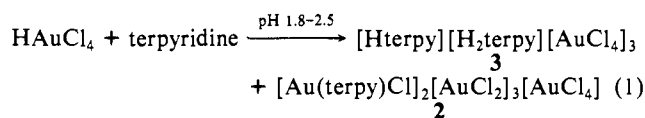
Figure 5. Stereoview of the unit-cell packing diagram for $[\text{Au}(\text{terpy})\text{Cl}]_2[\text{AuCl}_2]_3[\text{AuCl}_4]$ (**2**).

A stereoview of the packing of compound **2** in the crystal lattice is shown in Figure 5. The Au–Au distance [3.093 (1) Å] between the two unique gold atoms in the linear chain of $[\text{AuCl}_2]^-$ anions, situated between the $[\text{Au}(\text{terpy})\text{Cl}]^{2+}$ cations, is similar to the Au–Au distances found in a number of Au(I) complexes. For example, the structure of the polymeric dialkyldithiophosphate bridged digold(I) complex, $\{[\text{Au}(i\text{-C}_3\text{H}_7\text{O})_2\text{PS}_2]_2\}_n$,⁴⁰ which consists of a linear chain of $[\text{Au}(i\text{-PrO})_2\text{PS}_2]_2$ dimers that are stacked with a staggered conformation about the interdimer Au–Au vector, contains Au–Au distances that range from 2.914 (5) to 3.109 (6) Å. A similar linear chain arrangement of Au_2 molecules, which contain short Au(I)–Au(I) distances, is found in the structures of $[\text{ClAu}(\text{PhSCH}_2\text{CH}_2\text{SPh})\text{AuCl}]_n$,⁴¹ where the Au–Au distances are 3.187 (2)–3.209 (2) Å, and of $\{[(i\text{-C}_3\text{H}_7\text{NH}_2)\text{Au}(\text{C}\equiv\text{C}-\text{C}_6\text{H}_5)]_2\}_n$,⁴² where the Au–Au distances are 3.27 Å between the chains and 3.72 Å along the chain. The Au(I)–Au(I) distance in compound **2** is significantly longer than the Au–Au distances in gold metal, 2.884 Å,⁴³ and in the metal–metal bonded gold atoms in the cluster complexes $\text{Au}_{11}\text{X}_3(\text{PR}_3)_7$, 2.612 (4)–2.716 (4) Å.⁴⁴ Distances in the 3.0–3.1 Å range in Au(I) complexes indicate weak metal–metal interactions.⁴⁵

The enhanced positive charge in the $[\text{Au}(\text{terpy})\text{Cl}]^{2+}$ cation, compared to the corresponding complexes of Pt(II) and Pd(II), is probably responsible for its weak association with axial ligands such as Cl^- or H_2O . Such a feature is not observed in the structures of $[\text{Pd}(\text{terpy})\text{Cl}]\text{Cl}\cdot 2\text{H}_2\text{O}$ and $[\text{Pt}(\text{terpy})(\text{SCH}_2\text{CH}_2\text{OH})(\text{NO}_3)]$, where the planar cations are found to pack in layers within the unit cells.³ In the structure of the $[\text{Pd}(\text{terpy})\text{Cl}]^+$ complex, the cations pack in columnar stacks with an average interplanar separation of 3.4 Å. The closest approach to the axial sites of the Pd atom is 3.13 Å, to a nitrogen atom in an adjacent ring. The $[\text{Pt}(\text{terpy})(\text{SCH}_2\text{CH}_2\text{OH})]^+$ cation also stacks with overlapping terpyridine rings, and the closest axial contacts for the Pt atom in this molecule are to adjacent Pt [3.572 (8) Å] and N (3.60 Å) atoms in a neighboring cation. The fact that the planar $[\text{Au}(\text{terpy})\text{Cl}]^{2+}$ cation does not form stacked structures with interactions between adjacent rings suggests that

this complex may interact differently with DNA than the known metallointercalation reagents $[\text{Pt}(\text{terpy})(\text{SCH}_2\text{CH}_2\text{OH})]^+$ and $[\text{Pt}(\text{terpy})\text{Cl}]^+$. The DNA binding properties of $[\text{Au}(\text{terpy})\text{Cl}]^{2+}$ are presently being investigated.

Solution Chemistry of $[\text{Au}(\text{terpy})\text{Cl}]^{2+}$. The reaction between tetrachloroauric acid and terpyridine in aqueous solution yields a number of products. The pH of the solution during the reaction is important in determining the product distribution. The reactions between equimolar ratios of HAuCl_4 with terpyridine, as a function of pH, are summarized in eq 1–3. When the initial pH of the



reaction is adjusted in the range 1.8–2.5, the primary product is the tetrachloroaurate salt of mono- and diprotonated terpyridine (**3**). It should be noted that the identity of compound **3** is based solely on elemental analysis and its reaction with base to form **1**. The insolubility of **3** precluded the collection of confirmatory spectroscopic or conductometric data. While other formulations are conceivable, the double salt one used here is believed to be correct. Insoluble tetrachloroaurate salts of protonated amines are quite common.¹⁷ While terpyridine is found to form monoprotonated salts³² with $[\text{PtCl}_4]^{2-}$, the acidic conditions of the reaction promote the precipitation of the mixed $[\text{Hterpy}]^+$, $[\text{H}_2\text{terpy}]^{2+}$ salt of $[\text{AuCl}_4]^-$. The formation of the $[\text{H}_2\text{terpy}]^{2+}$ species under these conditions is expected on the basis of the weak basicity of terpyridine ($\text{p}K_1 = 4.7$ and $\text{p}K_2 = 3.3$).⁴⁶ A small amount (<5% yield) of the mixed-valent complex **2** is also obtained under these conditions. This product presumably results from the reduction of $[\text{AuCl}_4]^-$, or a related chloroquo species of Au(III),¹⁴ to form the $[\text{AuCl}_2]^-$ complex; the standard reduction potential for the $[\text{AuCl}_4]^-/[\text{AuCl}_2]^-$ couple is +0.926 V.⁴⁷ Although the mechanism of the redox process remains to be established, aqueous solutions of $[\text{AuCl}_4]^-$ have been found to undergo reduction to Au(I) and Au(0) in related reactions with amines.^{14,18} The mixed-valent complex $[\text{Au}(\text{dmg})_2][\text{AuCl}_2]$ is also produced in a

(37) (a) Elliot, N. *J. Chem. Phys.* **1934**, *2*, 419. (b) Elliot, N.; Pauling, L. *J. Am. Chem. Soc.* **1938**, *60*, 1846 (c) Arai, G. *J. Recl. Trav. Chim. Pays-Bas* **1962**, *81*, 307.

(38) Rundle, R. E. *J. Am. Chem. Soc.* **1954**, *76*, 3101.

(39) Dell'Amico, D. B.; Calderazzo, F.; Marchetti, F.; Merlino, S. *J. Chem. Soc., Chem. Commun.* **1977**, 31.

(40) Lawton, S. L.; Rohrbach, W. J.; Kokotailo, G. T. *Inorg. Chem.* **1972**, *11*, 2227.

(41) Drew, M. G. B.; Reidl, M. J. *J. Chem. Soc., Dalton Trans.* **1973**, 52.

(42) Corfield, P. W. R.; Shearer, H. M. M. *Acta Crystallogr.* **1967**, *23*, 156.

(43) Pauling, L. *The Nature of the Chemical Bond*, 3rd ed.; Cornell University Press: Ithaca, NY, 1960; p 410.

(44) Albano, V. G.; Bellon, P. L.; Manassero, M.; Sansoni, M. *J. Chem. Soc., Chem. Commun.* **1970**, 1210.

(45) Piovesana, O.; Zannazzi, P. F. *Angew. Chem., Int. Ed. Engl.* **1980**, *19*, 561.

(46) Offenhardt, P. O.; George, P.; Haight, G. P., Jr. *J. Phys. Chem.* **1963**, *67*, 116.

(47) Skibsted, L. H.; Bjerrum, J. *Acta Chem. Scand., Ser. A* **1977**, *A31*, 155.

similar fashion from the reaction of HAuCl_4 with dimethylglyoxime.³⁸

When the initial pH of the reaction is adjusted between 3 and 5, $[\text{Au}(\text{terpy})\text{Cl}]\text{Cl}_2 \cdot 3\text{H}_2\text{O}$ is obtained in good yield ($\sim 75\%$). The mixed-valent complex **2** is also a byproduct of this reaction ($\leq 5\%$ yield). When the pH of the reaction is initially adjusted to 7 or above, complete reduction to gold metal is observed. Formation of the metal must result from the reduction of $[\text{AuCl}_4]^-$ since solutions of $[\text{Au}(\text{terpy})\text{Cl}]\text{Cl}_2$ are stable under these conditions.

The aqueous solution chemistry of $[\text{Au}(\text{terpy})\text{Cl}]^{2+}$ can be compared to that of the structurally analogous $[\text{Au}(\text{dien})\text{Cl}]^{2+}$ complex. The reaction between HAuCl_4 and dien similarly produces a variety of products as a function of pH.¹⁸ In the low pH range (< 2), the tetrachloroaurate salt of dien, $[\text{H}_3\text{dien}][\text{AuCl}_4]$, is produced in a reaction which resembles reaction 1. When the reaction is carried out at $\text{pH} \sim 4$, the main product is the $[\text{Au}(\text{dien})\text{Cl}][\text{AuCl}_4]_2$ salt. Although the analogous $[\text{Au}(\text{terpy})\text{Cl}][\text{AuCl}_4]_2$ complex has yet to be isolated, it is possible that this product is one of the unidentified materials obtained in small quantities from reaction 1.

Conclusion

The structure of the cation in $[\text{Au}(\text{terpy})\text{Cl}]\text{Cl}_2 \cdot 3\text{H}_2\text{O}$ is similar to those of the analogous terpyridine complexes of Pd(II) and Pt(II). The planar $[\text{Au}(\text{terpy})\text{Cl}]^{2+}$ cation contains elongated axial

ligand contacts to H_2O and Cl^- in the crystal lattice, however, and does not form a stacked arrangement of planar cations as found in the structures of the related Pd(II) and Pt(II) complexes. The chemistry of $[\text{Au}(\text{terpy})\text{Cl}]^{2+}$ in water resembles that of the structurally analogous Au(III) complex of diethylenetriamine, $[\text{Au}(\text{dien})\text{Cl}]^{2+}$. The insoluble mixed-valent Au(III)-Au(I) compound $[\text{Au}(\text{terpy})\text{Cl}]_2[\text{AuCl}_2]_3[\text{AuCl}_4]$, which forms as a byproduct of the reaction used to prepare $[\text{Au}(\text{terpy})\text{Cl}]^{2+}$, is composed of a chain of three linear $[\text{AuCl}_2]^-$ anions that link two $[\text{Au}(\text{terpy})\text{Cl}]^{2+}$ cations through long axial, Au(III)-Au(I), contacts. The $[\text{Au}(\text{terpy})\text{Cl}]^{2+}$ cations in the mixed-valent salt are further linked together through axial interactions to the chlorine atoms of the square-planar $[\text{AuCl}_4]^-$ anion.

Acknowledgment. This work was supported by National Institutes of Health Research Grant CA-15826 from the National Cancer Institute. We thank Paul Chang for experimental assistance.

Registry No. 1, 85719-47-7; 2, 85709-76-8; 3, 85709-77-9.

Supplementary Material Available: Atomic positional and thermal parameters for compounds **1** and **2** (Tables S1 and S2) as well as final observed and calculated structure factors (Tables S3 and S4) (31 pages). Ordering information is given on any current masthead page.

Studies in Aromatic Nitration. 2.¹ ¹⁴N NMR Study of the Nitric Acid/Nitronium Ion Equilibrium in Aqueous Sulfuric Acid

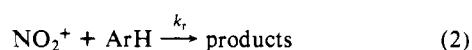
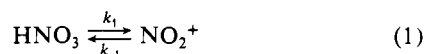
David S. Ross,* Karl F. Kuhlmann, and Ripudaman Malhotra

Contribution from the Physical Organic Chemistry Department, SRI International, Menlo Park, California 94025. Received August 11, 1982

Abstract: The nitric acid/nitronium ion equilibrium at 25 °C in aqueous sulfuric acid (81–96%) has been studied by ¹⁴N NMR spectroscopy. In contrast to observations by Seel et al. (1972), who obtained only one NMR signal, we observed separate signals for nitric acid and nitronium ion. A 50% conversion of added nitric acid into nitronium ion is observed in 88% sulfuric acid, a value in good agreement with that obtained by others using Raman spectroscopy. From the line-shape analysis of these spectra, pseudo-first-order rate constants for the formation and hydration of nitronium ion were obtained. Examination of these data reveals certain inconsistencies between the currently accepted mechanism and observed rates and orders of aromatic nitration.

We present here the results of our investigation of nitric acid/nitronium ion equilibrium using ¹⁴N NMR spectroscopy. Our findings reveal inconsistencies between the accepted mechanism and the observed rates and orders of aromatic nitration. The classical studies of Ingold and Co-workers² established that nitration of aromatic compounds in nitric acid-sulfuric acid mixtures proceeds through the intermediacy of the nitronium ion (Scheme I), where k_1 and k_{-1} are respectively the pseudo-first-

Scheme I



order rate constants for the formation and hydration of nitronium ion and k_r is the specific rate of reaction of the nitronium ion with the aromatic substrate. The formalism used in this paper is that of Moodie, Schofield, and Taylor.³

Nitric acid in an acid-catalyzed step is first reversibly transformed into nitronium ion, which then reacts with the aromatic to form products. Such a scheme leads to the following rate expression for the formation of nitro products:

$$\text{rate} = \frac{k_1 k_r [\text{ArH}] [\text{HNO}_3]}{k_{-1} + k_r [\text{ArH}]} \quad (3)$$

An independent determination of the rate constants k_1 and k_{-1} is thus of crucial importance to the mechanism of aromatic nitration.

(1) Part I: Schmitt, R. J.; Ross, D. S.; Buttrill, S. E., Jr. *J. Am. Chem. Soc.* **1981**, *103*, 5365–5267.

(2) Ingold, C. K. "Structure and Mechanism in Organic Chemistry"; 2nd ed.; Cornell University Press: Ithaca, NY, 1969.

(3) Moodie, R. B.; Schofield, K.; Taylor, P. G. *J. Chem. Soc., Perkin Trans. 2* **1979**, 133–136.